MetaResource vol. XX, no. X, pp. 1–XX, 202X
DOI: 10.23919/METAR.2026.000060
Original Article

Calculation method of sectional velocity and coal flow based on discrete element simulation for scraper conveyors

Qiang Zhang[1], Anhao Jia[1], Wei Liu[1,✉], Yingbo Liu[2], and Zhengyang Wang[1]

[1] *Shandong University of Science and Technology, Qingdao 266000, China*
[2] *Zhuhai Port Holding Group Co., Ltd., Zhuhai 519050, China*

Received: 14 Feb 2026
Revised: 27 May 2026
Accepted: 4 Jun 2026
Online: xx xxx xxxx

KEYWORDS

scraper conveyor,
coal flow,
sectional velocity domain,
discrete element simulation,
data fitting

ABSTRACT

To address the limitation that traditional coal flow calculation methods based on the sectional average-velocity assumption cannot reflect the non-uniform velocity distribution of coal flow in the middle trough of scraper conveyors, this paper proposes a coal flow calculation method based on sectional velocity-domain statistics. In this method, the non-uniform velocity field obtained from discrete element method (DEM) simulations is converted into area-based velocity-domain parameters, and these parameters are further combined with scraper structural parameters to establish an explicit coal flow calculation model. This provides a computational basis for conveying capacity evaluation and operating parameter matching of scraper conveyors. Firstly, a coal flow transport model for the middle trough of three scraper conveyor width models (SGB800, SGB1000, and SGB1250) was established based on the discrete element method. The velocity distribution characteristics of coal flow within the conveyor cross-section were systematically analyzed under different scraper chain speeds and coal pile heights. Based on the differences in chain speeds, the sectional velocity was divided into domains, and the area of each velocity zone was statistically analyzed. The representative velocity for each zone was used to perform an equivalent calculation of the indirect transport volume. Additionally, a direct transport volume model was established in conjunction with scraper structural parameters, thereby forming a coal flow calculation expression applicable to mainstream trough widths, chain speeds, and coal pile height conditions. Finally, the calculation results were verified through scaled experiments. The results showed that the calculated values

Address correspondence to Wei Liu: j1876665@qq.com
© The author(s) 2026. The articles published in this open access journal are distributed under the terms of the Creative Commons Attribution 4.0 International License (http://creativecommons.org/licenses/by/4.0/).

有斛出版 YOUKE PUBLISHING EXCLUSIVELY AVAILABLE VIA IEEE Xplore DIGITAL LIBRARY

were in good agreement with the experimental results, with the maximum error in the experimental comparison not exceeding 10%. This provides a reliable theoretical and engineering calculation method for the evaluation of scraper conveyor capacity, parameter matching, and operational safety analysis.

1 Introduction

In the context of the coal industry's transition toward intelligent, high-yield, and high-efficiency operations, the continuous production capacity of fully mechanized mining faces relies heavily on the stable operation and precise control of the transportation system. As a core transportation equipment, the conveying capacity of scraper conveyors directly determines the production efficiency and equipment reliability of the working face. Among them, coal flow rate is a key indicator of conveying capacity and working condition matching. Accurate and rapid calculation of coal flow is an essential foundation for optimizing the design of the transportation system, performing online status assessments, and providing fault warning systems [1–3].

From the perspective of the dynamics and operational safety of scraper conveyors, coal flow not only represents the material conveying capacity but also serves as the primary source of mechanical load for the system. Its spatial-temporal distribution and fluctuations directly affect the dynamic tension level of the chain, the vibration response of the transmission system, and the overall operational stability of the machine [4, 5]. Existing studies in China and abroad, based on vibration analysis and dynamic modeling methods, have revealed the mechanism of abrupt changes in chain speed and contact force under abnormal conditions such as chain jamming and chain breakage [6–8]. These studies indicate that such abnormalities can significantly amplify impact loads, posing a severe threat to system safety. These abnormal conditions are rarely incidental; their triggering factors can typically be traced back to local abrupt changes in coal flow, abnormal accumulation, or uneven load distribution, which cause a sudden increase in resistance and dynamic instability. Therefore, accurate characterization and monitoring of coal flow are key foundations for analyzing dynamic behavior and enhancing operational safety.

In terms of research methods, the discrete element method (DEM) has been widely used to investigate bulk material transport systems because it can describe particle-scale contact, collision, sliding, accumulation, and stratification. Recent studies have shown that DEM has become an important tool for analyzing powder and bulk-material transport systems, such as screw feeders, screw conveyors, transfer chutes, and other conveying equipment [9–12]. Ilic et al. [13] used DEM to predict screw conveyor performance and analyzed particle velocity, mass flow rate, energy dissipation, and power consumption, demonstrating the applicability of DEM in engineering-oriented bulk-material conveying analysis. In addition to its direct application in bulk-material conveying simulations, DEM also provides an effective basis for multiscale modelling because particle-scale information can be transformed into mesoscopic or continuum-scale parameters through discrete-to-continuum or coarse-graining methods [14]. This concept supports the present study, in which the DEM-derived particle velocity field is converted into sectional velocity-domain area parameters for coal flow calculation.

For scraper conveyors, existing DEM-based studies have mainly focused on the interaction between bulk coal, scraper chains, and the middle trough. Wang et al. [15] investigated the bulk coal transport state of a scraper conveyor using DEM and reported that coal particles in the middle trough did not move as a uniform body. Particles close to the scraper move at a velocity close to the chain speed, whereas particles in the upper layer and near the side regions move more slowly. This indicates that coal flow in the middle trough has obvious velocity stratification and regional differences. In addition, coupled DEM–MBD/DEM–FEM methods have been used to study the dynamic response and load transfer of scraper conveyors under chain faults and abnormal operating conditions [16].

DEM-based studies have also been conducted to analyze chute wear and middle-trough wear behavior caused by coal particle motion, particle size stratification, and coal–structure contact [17–20]. Moreover, impact damage to the middle trough has been investigated by considering the effects of particle size, velocity, and impact conditions [21].

Although these studies have provided important insights into coal particle motion, load response, wear evolution, and structural damage, most of them use DEM results mainly for mechanism interpretation, parameter influence analysis, or local mechanical-effect evaluation. The simulation results are usually discussed in the form of velocity contours, particle trajectories, contact forces, or wear distributions. Relatively few studies have further transformed the DEM-derived non-uniform sectional velocity field into quantitative parameters for engineering coal flow calculation.

At present, coal flow estimation for scraper conveyors still commonly relies on the assumptions of uniform material motion or sectional average velocity. These assumptions cannot distinguish the different contributions of high-velocity and low-velocity regions to the total coal flow, and may therefore lead to deviations in conveying capacity evaluation and operating parameter matching when velocity stratification, local accumulation, and particle shear motion occur in the middle trough.

To address these limitations, this study proposes an engineering-oriented coal flow calculation method based on sectional velocity-domain statistics. The proposed method establishes a quantitative connection between the DEM-derived non-uniform sectional velocity field and coal flow calculation. The sectional velocity field is divided into several velocity domains according to the scraper chain speed, and the indirect conveying component is calculated using velocity-domain area statistics, while the direct conveying component generated by scraper pushing is incorporated according to scraper structural parameters. In this way, the non-uniform velocity field of coal particles is transformed into explicit geometric and kinematic parameters for rapid coal flow estimation under different trough widths, scraper chain speeds, and coal pile heights.

2 Discrete element simulation of coal flow

The coal flow in a scraper conveyor is a typical discrete bulk material conveying problem. Its motion process involves significant inter-particle contact, collision, accumulation, and sliding behaviors, which are difficult to accurately describe using the assumption of a continuous medium [22]. DEM treats coal as a large number of interacting discrete particles, enabling the mechanical behavior between particles and between particles and structures to be characterized at the microscopic scale, thereby reflecting the overall conveying characteristics of coal flow at the macroscopic level [23]. Therefore, employing DEM to conduct numerical simulation of coal flow in scraper conveyors is an important approach for investigating the motion mechanism of coal flow and the conveying capacity.

In this study, a coal flow conveying model of a scraper conveyor is established based on the DEM. Through numerical simulation of the motion process of coal particles within the middle trough, the velocity distribution of coal flow, spatial accumulation patterns, and cross-sectional characteristics under steady operating conditions are obtained. On this basis, a reliable data foundation is provided for subsequent analysis of coal flow velocity stratification and calculation of conveying capacity.

2.1 Fundamental theory of DEM

DEM, originally proposed by Cundall and Strack for modeling granular assemblies [24], is a numerical method for discontinuous media mechanics, particularly suitable for simulating the motion and interactions of bulk particulate materials, such as crushed coal and rock. It discretizes the object being modeled into a series of independent rigid or deformable particle units, and simulates the overall macroscopic mechanical behavior by tracking the motion of each unit and the contact forces between them [25].

The core idea of DEM is based on Newton's second law. At each time step, for every particle in the system, the acceleration is calculated based on all the forces acting on it (such as contact forces and body

forces), and then its velocity and position are updated through time integration [26]. This iterative calculation process continues, simulating the dynamic evolution of the entire system.

For any particle i, its translational and rotational motions are described by the following equation:

$$\begin{aligned} m_i \frac{\mathrm{d}^2 u_i}{\mathrm{d}t^2} &= \sum\nolimits_j F_{ij}^c + F_i^g \\ I_i \frac{\mathrm{d}w_i}{\mathrm{d}t} &= \sum\nolimits_j M_{ij} \end{aligned} \tag{1}$$

where m_i and I_i are the mass and moment of inertia of particle i, respectively. u_i and w_i are the displacement and angular velocity vectors of particle i, respectively. F_{ij}^c is the contact force exerted by particle j on particle i. F_i^g is the body force (such as gravity) acting on particle i. M_{ij} is the torque generated by the contact force F_{ij}^c.

The calculation of contact forces is the core of DEM. The most commonly used contact model is the Hertz-Mindlin contact model. This contact model is the default contact model in EDEM software and serves as the fundamental contact model for discrete element simulations in EDEM [27].

To further illustrate the interaction mechanism between coal particles, a schematic diagram of the particle contact model and contact-force representation is presented in Figure 1 [28]. In DEM calculations, coal particles are treated as discrete particle units. When particle i comes into contact with particle j under inertia or external force, local contact deformation occurs during their relative motion. In the soft-sphere contact model, the detailed deformation process at the contact region is not explicitly resolved; instead, the normal overlap α and tangential displacement δ are used to calculate the contact forces between particles. The contact force can be further decomposed into normal and tangential components, which are commonly represented by equivalent spring, dashpot, and frictional sliding elements. This contact model provides a physical basis for describing inter-particle collision, friction, and momentum transfer in coal flow.

Assume that two spherical particles with radii R_1 and R_2 undergo elastic contact. The equations for calculating the normal overlap α and the contact radius a of the interface between the two spherical particles are as follows:

$$\begin{aligned} \alpha &= R_1 + R_2 - |r_1 - r_2| \\ \mathrm{a} &= \sqrt{\alpha R^*}, \qquad \frac{1}{R^*} = \frac{1}{R_1} + \frac{1}{R_2} \end{aligned} \tag{2}$$

where r_1 and r_2 are the position vectors of the centers of the two spherical particles; R^* is the equivalent particle radius.

The calculation equations for the normal force F_n and the normal damping force F_n^d between particles are as follows:

$$\begin{aligned} F_\mathrm{n} &= \frac{4}{3} E^* (R^*)^{\frac{1}{2}} \alpha^{\frac{3}{2}}, \frac{1}{E^*} = \frac{1-\mathrm{v}_1^2}{E_1} + \frac{1-\mathrm{v}_2^2}{E_2} \\ F_\mathrm{n}^\mathrm{d} &= -2\sqrt{\frac{5}{6}} \beta \sqrt{S_\mathrm{n} m^*}\, v_\mathrm{n}^\mathrm{rel}, \quad m^* = \frac{m_1 m_2}{m_1 + m_2} \end{aligned} \tag{3}$$

where E^* is the equivalent elastic modulus; E_1 and E_2 are the elastic moduli of particles 1 and 2, respectively; v_1 and v_2 are the Poisson's ratios of particles 1 and 2; β is the normal coefficient; m^* is the equivalent mass; m_1 and m_2 are the masses of particles 1 and 2, respectively.

Assuming the velocities of the two particles before

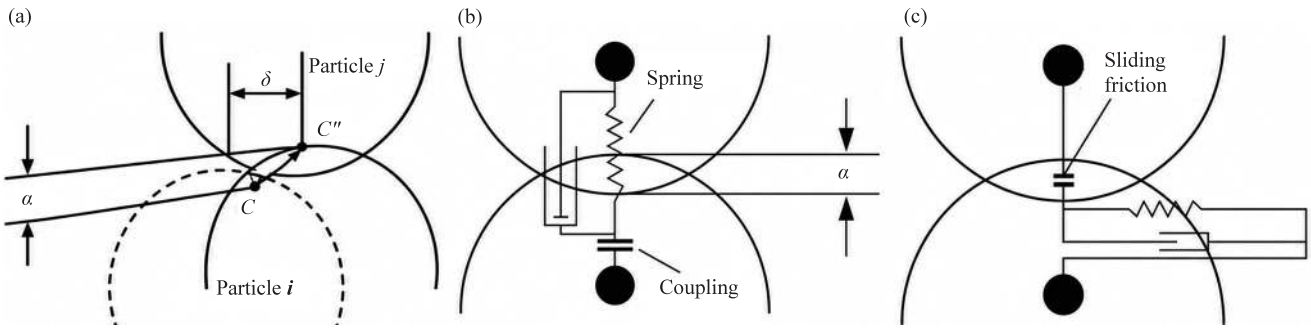

Figure 1 Contact relationship and contact-force model between coal particles in DEM: (a) soft-sphere model of two contacting particles; (b) simplified normal-force model; (c) simplified tangential-force model

collision are v_1 and v_2, the calculation equations for the normal coefficient β, the tangential force F_t, and the tangential damping force F_t^d between the particles during the collision are as follows:

$$\beta = \frac{\ln e}{\sqrt{\ln^2 e + \pi^2}} \tag{4}$$

$$F_t = -S_t \delta, \quad S_t = 8G^* \sqrt{R^* \alpha}$$
$$G^* = \frac{2-\nu_1^2}{G_1} + \frac{2-\nu_2^2}{G_2} \tag{5}$$

$$F_t^d = -2\sqrt{\frac{5}{6}}\beta \sqrt{S_t m^*} v_t^{rel} \tag{6}$$

where e is the restitution coefficient, which describes the energy recovery ability after collision. A smaller e indicates stronger energy dissipation and weaker rebound. δ is the tangential overlap; S_t is the tangential stiffness; G^* is the equivalent shear modulus; G_1 and G_2 are the shear moduli of particles 1 and 2, respectively; v_t^{rel} is the tangential relative velocity. These parameters are used to describe the tangential contact force, shear interaction, and tangential damping between particles.

The tangential force is limited by the Coulomb friction force $\mu_s F_n$, where μ_s is the static friction coefficient. It controls the tangential resistance between particles or between particles and the trough surface, thereby affecting particle sliding and accumulation. Rolling friction is introduced to describe the rotational resistance of particles and can be characterized by the torque on the contact surface:

$$T_t = -\mu_r F_n R_i w_i \tag{7}$$

where μ_r is the rolling friction coefficient; R_i is the distance from the particle centroid to the contact point; w_i is the unit angular velocity vector at the contact point. The rolling friction coefficient affects particle rotation, mobility, and velocity stratification, especially when irregular coal particles are simplified as spheres.

2.2 Establishment of the discrete element model

To analyze the influence of scraper conveyor specifications on coal flow, it is necessary to establish models of middle troughs with different specifications. In this study, three-dimensional models of SGB800, SGB1000, and SGB1250 width types were constructed using SolidWorks, and then imported into Altair EDEM, a commercial DEM software for bulk and granular material simulation, for subsequent numerical simulation analysis. The imported models are shown in Figure 2.

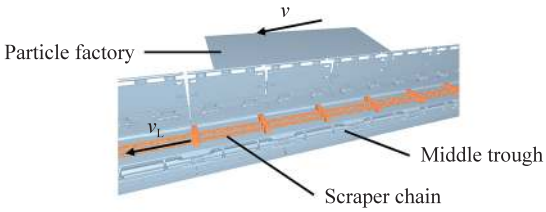

Figure 2 Discrete element model of the middle trough

To effectively simulate the transport process of lump coal within the scraper conveyor while ensuring computational efficiency, this study reasonably simplified the complex and irregular coal particles. The specific simplification scheme is as follows: The particle geometry is uniformly simplified to spheres to significantly reduce the complexity of contact detection and force calculations; the particle size is set to a nominal diameter of 20 mm, based on the particle size distribution in actual production. To represent the inherent heterogeneity of the material size distribution, the final diameter of each particle is randomly generated within a range of 0.9–1.3 times the nominal diameter, and the particle mass is automatically calculated from its generated diameter and the material density.

Since spherical particles cannot directly represent the angular morphology of actual lump coal particles and the resulting rotational resistance effects, this study introduces a relatively large rolling friction coefficient to equivalently account for the inhibition of particle rotation and rolling caused by the irregular shape of coal particles. The contact mechanics between particles are described using the Hertz-Mindlin contact model, with the relevant material and contact parameters listed in Tables 1–3. Through the combination of the spherical assumption, size randomization, and rolling friction compensation, the transport behavior of lump coal assemblies is effectively simulated within an acceptable computational cost.

It should be noted that the spherical particle assumption is a computational simplification. Compared with

Table 1 Material properties of coal

Parameter name	Symbol	Value	Unit
Poisson's ratio	v	0.25	—
Solid density	ρ	1400	kg/m^3
Shear modulus	G	3.0×10^9	Pa
Young's modulus	E	7.5×10^9	Pa

Table 2 Material properties of middle trough steel

Parameter name	Symbol	Value	Unit
Poisson's ratio	v	0.27	—
Solid density	ρ	7850	kg/m^3
Shear modulus	G	8.0×10^{10}	Pa
Young's modulus	E	2.032×10^{11}	Pa

Table 3 Contact parameter settings

Contact type	Restitution coefficient	Static friction coefficient	Rolling friction coefficient
Coal–coal	0.2	0.5	0.4
Coal–middle trough steel	0.2	0.5	0.5

real angular coal particles, spherical particles may underestimate particle interlocking and shape-induced resistance, which may lead to smoother particle motion and slightly higher local mobility. In this study, the rolling friction coefficient was introduced to compensate for the rotational resistance caused by the irregular shape of lump coal. However, this treatment cannot fully reproduce the geometric interlocking and angular contact behavior of real coal particles. Therefore, the calculated coal flow in this study should be regarded as an equivalent engineering estimate under the adopted contact parameters rather than a complete reproduction of the motion of every irregular coal particle.

To investigate the transport characteristics of lump coal in the scraper conveyor under different operating conditions, multiple typical working scenarios were simulated numerically. The scraper chain speeds were set to v = 0.8, 1.0, 1.2, 1.4, and 1.6 m/s, covering both common and relatively high operating speeds of underground scraper conveyors, thereby systematically examining the influence of chain speed variation on lump coal transport behavior. For the middle trough models of SGB800, SGB1000, and SGB1250 with different widths, simulations were conducted under the five aforementioned scraper chain speeds. Each trough model was thus analyzed under five chain speed conditions, resulting in a total of 15 discrete element simulation cases. Comparative analysis across multiple operating conditions and structural combinations enables an effective investigation on the effects of trough width and scraper chain speed on coal flow.

For the initial coal loading conditions, the coal pile height within each middle trough was appropriately determined based on the dimensions of the coal baffle corresponding to the trough width, ensuring that all models have comparable and practically meaningful loading states. Given the pronounced zonal characteristics of coal particle velocity within the conveying cross-section, with significantly reduced flow speeds near the sides of the middle trough, boundary conditions with coal baffles installed on both sides of the trough were adopted in this study. This prevents near-stagnant regions from being included in the statistics, thereby preserving the comparability between different models. Considering both the structural height from the top of the coal baffle to the wear-resistant surface of the middle trough and the typical loading levels during scraper conveyor operation, the coal pile height was finally set to 1.40 m for the SGB800 middle trough, and 1.50 m for both the SGB1000 and SGB1250 middle troughs.

Through the combination of the above operating conditions and loading settings, a reliable simulation foundation was established for subsequent analysis of lump coal transport efficiency, motion characteristics, and structural adaptability within the scraper conveyor, while maintaining computational efficiency.

In the numerical simulation, the initial coal loading was implemented using a gravity-driven drop method. Specifically, coal particles were continuously released above the middle trough, allowing them to fall freely under gravity and naturally accumulate within the trough. The release was stopped once the coal pile reached the predetermined height, thereby establishing an initial particle accumulation state consistent with actual operating conditions.

The scraper chain was then activated, causing the

particles to transition from the initially stationary pile to a transported state driven by the scraper. During the initial start-up of the scraper, the particle system underwent a transient adjustment period, during which the overall motion had not yet stabilized; this stage was excluded from the statistical analysis. Once the system reached steady-state operation, the overall motion characteristics and velocity distribution of the particles became stable. Kinematic parameters such as particle velocity were then statistically analyzed during this stable stage to characterize the transport behavior of lump coal within the scraper conveyor under different operating conditions.

To improve the standardization and repeatability of the DEM simulations, the main numerical settings and post-processing criteria were specified. The simulations were conducted using EDEM, and the Euler explicit integration scheme was adopted. The automatic time-step option was enabled; therefore, the physical integration time step was automatically controlled by EDEM according to particle size, material properties, contact stiffness, and numerical stability requirements. The simulation results were saved at a target output interval of 0.1 s for subsequent velocity-field extraction and cross-sectional area statistics.

In the statistical analysis, the transient start-up stage was excluded. After the coal flow reached a stable conveying state, the sectional velocity field was extracted at the same cross-section for all working conditions. The calculation stability was evaluated based on the coal accumulation profile, sectional velocity distribution, and outlet flow variation. When these quantities showed no obvious continuous increase or decrease, the corresponding data were used for subsequent velocity-domain area statistics and coal flow calculation.

3 Coal flow calculation method based on sectional velocity domain statistics

3.1 Velocity domain partitioning and area statistical method

Under the limiting coal loading condition, the coal flow within the middle trough reaches its maximum loading state. The resulting coal flow rate and conveying capacity can therefore be regarded as the "capacity boundary" of the equipment for selection verification and operating condition constraints. Under this boundary condition, the total coal flow conveying capacity was calculated based on the sectional statistics of the velocity field within the conveying cross-section. Comparative analyses were then conducted under different trough widths and scraper chain speeds.

Previous studies have considered the influence of sectional area and regional velocity distribution on the transport capacity of scraper conveyors. Ren et al. [29] divided the load cross-section into several regions, assigned different velocity ratios according to the relative position of each region with respect to the scraper chain, and calculated the conveying capacity by combining regional area, velocity ratio, chain speed, and coal bulk density. This provides an engineering calculation route based on sectional-area weighting, but the velocity ratios are mainly obtained from empirical assumptions. In addition, DEM-based studies have visualized the velocity distribution of bulk coal in the middle trough and shown that particles in the central region generally move faster than those near the side regions. Therefore, it is necessary to further convert the DEM-derived non-uniform velocity field into quantitative velocity-domain area parameters for coal flow calculation.

After the simulation reached steady-state operation, the velocity distribution data of the coal flow within the conveying cross-section were exported and used as the fundamental input for subsequent flow rate calculations. Due to the pronounced non-uniformity of the sectional velocity field, directly adopting an average velocity would obscure the different contributions of local high-velocity and low-velocity regions to the total flow rate. Therefore, a velocity domain area statistical method was employed, in which the velocity field was discretized into a finite number of velocity layers, and the area proportion of each velocity layer within the cross-section was statistically determined.

Using the chain speed v as the reference scale, the sectional velocity range was divided into four layers, and the corresponding domain areas were defined accordingly. S_1 denotes the conveying cross-sectional area corresponding to velocities within $1.0v$–$0.8v$; S_2 corresponds to $0.8v$–$0.6v$; S_3 corresponds to $0.6v$–$0.4v$;

S_4 corresponds to 0.4v–0.2v. In the regular colored region on the left side of the velocity-domain figure, the red region represents the statistical area of S_1; the green region represents the statistical area of S_2, and the yellow region represents the statistical area of S_3. The remaining uncolored region within the effective coal-flow cross-section is defined as S_4. Its area was obtained by subtracting the colored statistical areas of S_1, S_2, and S_3 from the total effective coal-flow cross-sectional area determined by the coal pile height and middle trough width. Regions with velocities lower than 0.2v were excluded from the statistical analysis because their contribution to the total coal flow rate is negligible. The velocity-domain partitioning is illustrated in Figure 3.

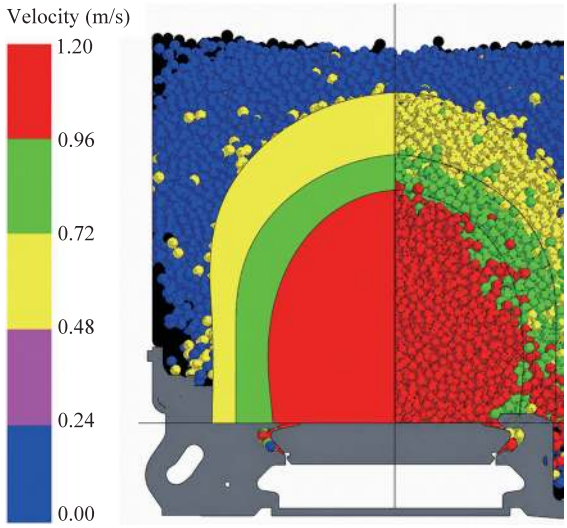

Figure 3 Velocity domain partitioning of the SGB1000 middle trough at a chain speed of 1.2 m/s

3.2 Coal flow calculation method

The total coal throughput (mass flow rate) consists of two components. The first is the indirect volumetric flow rate, which is associated with the bulk motion of the coal bed above the scraper driven by particle collisions and shear-induced movement. The second is the direct volumetric flow rate, which is generated by the scraper pushing coal directly. Accordingly, the total coal mass flow rate (t/h) can be written as

$$Q_{\text{tot}} = \frac{\rho_{\text{b}}\left(V_{\text{mid}} + V_{\text{scr}}\right)\times 3600}{1000} \tag{8}$$

where ρ_{b} is the bulk density of coal, taken as 850 kg/m^3; V_{mid} is the indirect volumetric flow rate above the scraper that is not directly pushed by the scraper (m^3/s); V_{scr} is the direct volumetric flow rate produced by the scraper's direct pushing action (m^3/s).

The indirect transport volume originates from the overall flow of coal above the scraper. To convert the non-uniform velocity field into a calculable form, a representative velocity was assigned to each velocity interval, taking the median value of the interval as the equivalent transport velocity for that layer. For the four velocity layers S_1–S_4, the equivalent velocities can be expressed as

$$u_1 = 0.9v, u_2 = 0.7v, u_3 = 0.5v, u_4 = 0.3v \tag{9}$$

The indirect transport volumetric flow rate is calculated as the sum of "area × equivalent velocity" for each velocity domain:

$$V_{\text{mid}} = S_1u_1 + S_2u_2 + S_3u_3 + S_4u_4 = 0.9v\cdot S_1 + 0.7v\cdot S_2 + 0.5v\cdot S_3 + 0.3v\cdot S_4 \tag{10}$$

where S_1–S_4 are the cross-sectional areas of the respective velocity domains, and v is the scraper operating speed.

The direct transport volume is related to the scraper's structural parameters, specifically the pushing area and pushing speed of the scraper. It can be calculated using the following equation:

$$V_{\text{scr}} = S_{\text{scr}} \times \left(\frac{L_1 - L_2}{L_1}\right) \times k \bullet v \tag{11}$$

where S_{scr} is the scraper pushing area (m^2); L_1 is the scraper pitch (m); L_2 is the scraper thickness (m); k is a reduction factor. Considering the relative slip between the coal mass in the scraper pushing zone and the scraper, as well as the velocity loss caused by inter-particle shear, the direct transport volume is corrected by the reduction factor k based on the ideal geometric pushing volume. A value of k = 0.9 was adopted to provide a conservative adjustment of the direct transport volume.

This method converts the non-uniform velocity field into verifiable geometric statistics, enabling a unified calculation of coal flow under different trough widths

and chain speeds. It provides standardized input and a computational basis for comparative analysis of conveying capacity and the development of empirical fitting formulas.

3.3 Sensitivity analysis of DEM contact parameters

To evaluate the dependence of the proposed coal flow calculation method on DEM contact parameters, a sensitivity analysis was conducted after establishing the sectional velocity-domain statistical method. The SGB1000 middle trough at a scraper chain speed of 1.2 m/s was selected as the representative working condition. The coefficient of restitution e, static friction coefficient μ_s, and rolling friction coefficient μ_r were varied independently by ±20% from their baseline values, while the other parameters were kept unchanged. For each sensitivity case, the sectional velocity-domain areas were recalculated using the same statistical procedure, and the corresponding coal flow rate was obtained according to the proposed calculation equation.

The baseline coal flow rate under the representative condition was 5166.10 t/h. To quantify the influence of each DEM contact parameter, the relative change in coal flow rate was calculated as

$$\eta_i = \frac{Q_i - Q_0}{Q_0} \times 100\% \tag{12}$$

where η_i is the relative change in coal flow rate; Q_0 is the baseline coal flow rate; Q_i is the coal flow rate obtained under each sensitivity case.

The results show that the calculated coal flow rate varies within a limited range under the ±20% variation of the DEM contact parameters. Compared with the baseline value, the maximum relative change is −4.47%, which occurs when the coefficient of restitution is increased by 20%. The variations caused by the static friction coefficient and rolling friction coefficient are within −0.93% to +0.35% and −0.74% to +0.36%, respectively. This indicates that although the DEM contact parameters influence local particle motion and velocity-domain distribution, the calculated coal flow rate remains relatively stable within the tested parameter range. Therefore, the proposed sectional velocity-domain statistical method has acceptable robustness with respect to reasonable variations in DEM contact parameters.

4 Coal flow calculation

4.1 Verification of DEM simulation results before model construction

Before the DEM simulation results were used to establish the coal-flow prediction functions, a scaled DEM model was established and verified using the scaled experimental platform. The scaled DEM model was built according to the 1:2 experimental platform of the SGB1000 scraper conveyor. The same chute geometry, coal pile height, and scraper chain speed were used in both the scaled DEM simulation and the scaled experiment.

Due to the limitations of the experimental conditions, the maximum achievable coal pile height of the scaled experimental platform was approximately 0.30 m. To ensure stable coal accumulation and avoid excessive boundary effects at very low pile heights, a representative scaled coal pile height of 0.250 m was selected for validation. According to the geometric similarity ratio of λ = 0.5, this height corresponds to a prototype coal

Table 4 Sensitivity analysis of DEM contact parameters based on the SGB1000 middle trough at v = 1.2 m/s

Case	Varied parameter	Variation	Coal flow rate, Q (t/h)	Relative change (%)
Baseline	—	—	5166.1	—
e−20%	Coefficient of restitution e	−20%	5193.753	0.54
e+20%	Coefficient of restitution e	20%	4935.118	−4.47
μ_s−20%	Static friction coefficient μ_s	−20%	5184.268	0.35
μ_s+20%	Static friction coefficient μ_s	20%	5118.181	−0.93
μ_r−20%	Rolling friction coefficient μ_r	−20%	5184.502	0.36
μ_r+20%	Rolling friction coefficient μ_r	20%	5127.618	−0.74

pile height of 0.500 m. Three scraper chain speeds of 1.0, 1.2, and 1.4 m/s were selected to verify the scaled DEM model. The comparison between the scaled DEM simulation and the scaled experiment is shown in Table 5.

As shown in Table 5, the scaled DEM results agree well with the scaled experimental results. The relative errors of the three validation conditions range from 5.79% to 8.49%, with a maximum error of 8.49%. In both the DEM simulation and the experiment, the coal flow rate increases with increasing scraper chain speed under the representative coal pile height. This indicates that the scaled DEM model can reasonably reproduce the coal conveying process. Therefore, the DEM simulation results can be considered reliable before being used to establish the coal-flow prediction functions in the following sections.

4.2 Simulation results and data analysis

After the simulation under the limiting coal loading condition reached steady-state operation, the distribution data of coal flow velocity on the conveying cross-section were exported. Considering the large number of result plots, representative simulation results for the SGB1000 middle trough at various velocity layers, as well as results for all trough models at a chain speed of v = 1.2 m/s, are presented in Figures 4 and 5. The

Table 5 Comparison between scaled DEM simulation and scaled experiment

Case No.	Scaled coal pile height, h (m)	Prototype coal pile height, h (m)	Chain speed, v (m·s^{-1})	DEM coal flow rate, Q_{DEM} (t·h^{-1})	Experimental coal flow rate, Q_{exp} (t·h^{-1})	Relative error (%)
1	0.25	0.5	1	513.03	560.65	8.49%
2	0.25	0.5	1.2	627.94	672.12	6.57%
3	0.25	0.5	1.4	763.12	810.05	5.79%

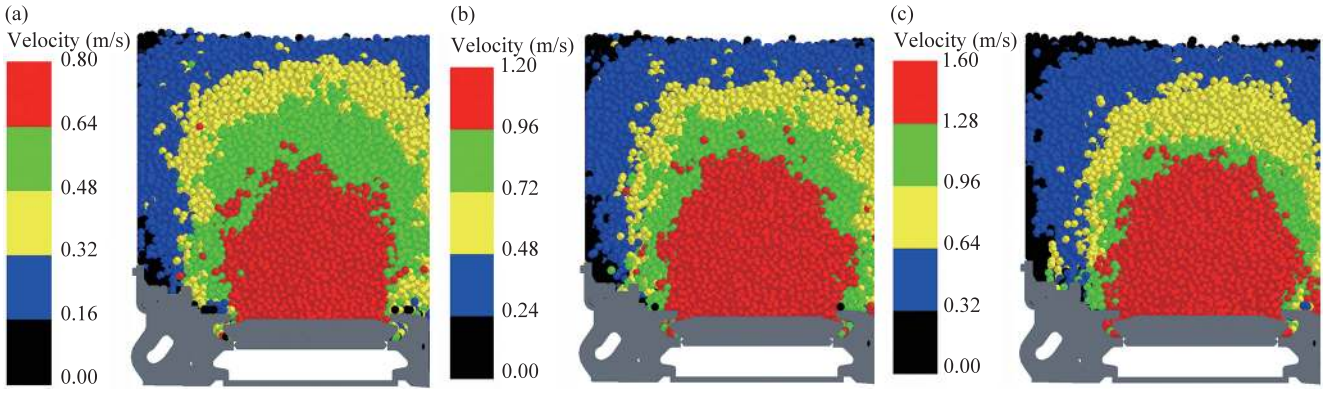

Figure 4 Simulation results of different velocity layers in the SGB1000 middle trough: (a) v = 0.8 m/s; (b) v = 1.2 m/s; (c) v = 1.6 m/s

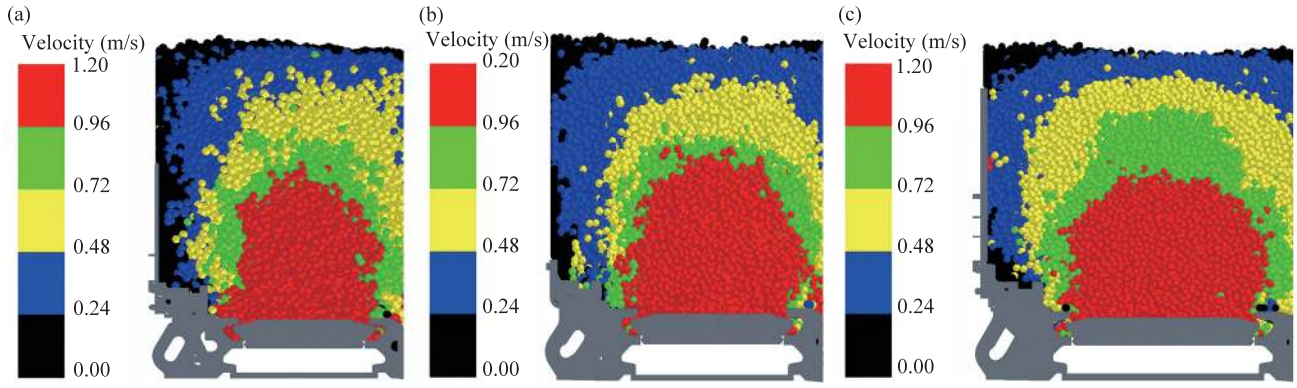

Figure 5 Simulation results of middle troughs with different widths at a chain speed of v = 1.2 m/s: (a) SGB800; (b) SGB1000; (c) SGB1250

statistical data from the simulations are summarized in Tables 6–8.

4.3 Coal flow calculation under limiting coal pile height

Under different chain speed conditions for various middle troughs, the indirect transport volume V_{mid}, direct transport volume V_{scr}, and total coal flow Q_{tot} of the scraper conveyor were calculated in detail, and the relevant transport results were statistically analyzed. The calculation results demonstrate the variation trends of coal flow in middle troughs of different widths and the impact of different scraper conveyor speeds on coal flow. The specific calculation results and statistical data are presented in Tables 9–11.

The calculated total coal flow values listed in

Table 6 Area statistics of velocity domains for different speeds in the SGB800 middle trough

Velocity	1.0v–0.8v (S1) (m^2)	0.8v–0.6v (S2) (m^2)	0.6v–0.4v (S3) (m^2)	0.4v–0.2v (S4) (m^2)	Total area (m^2) (S1 + S2 + S3 + S4)
v = 0.8 m/s	0.516548	0.296836	0.492578	0.589752	1.896
v = 1.0 m/s	0.600116	0.272842	0.384882	0.650436	1.908
v = 1.2 m/s	0.603178	0.26147	0.257094	0.780676	1.902
v = 1.4 m/s	0.603152	0.155992	0.265742	0.866617	1.892
v = 1.6 m/s	0.525928	0.206566	0.254876	0.876735	1.864

Table 7 Area statistics of velocity domains for different speeds in the SGB1000 middle trough

Velocity	1.0v–0.8v (S1) (m^2)	0.8v–0.6v (S2) (m^2)	0.6v–0.4v (S3) (m^2)	0.4v–0.2v (S4) (m^2)	Total area (m^2) (S1 + S2 + S3 + S4)
v = 0.8 m/s	0.667964	0.474536	0.508604	0.655896	2.307
v = 1.0 m/s	0.74898	0.37517	0.499966	0.647884	2.272
v = 1.2 m/s	0.7085	0.333716	0.468538	0.778246	2.289
v = 1.4 m/s	0.685926	0.336164	0.40871	0.8282	2.259
v = 1.6 m/s	0.64352	0.26989	0.416396	0.910194	2.240

Table 8 Area statistics of velocity domains for different speeds in the SGB1250 middle trough

Velocity	1.0v–0.8v (S1) (m^2)	0.8v–0.6v (S2) (m^2)	0.6v–0.4v (S3) (m^2)	0.4v–0.2v (S4) (m^2)	Total area (m^2) (S1 + S2 + S3 + S4)
v = 0.8 m/s	1.24769	0.479112	0.476574	0.553044	2.75642
v = 1.0 m/s	1.227874	0.500188	0.465816	0.572208	2.766086
v = 1.2 m/s	1.044374	0.59482	0.51478	0.632242	2.786216
v = 1.4 m/s	1.132332	0.372868	0.486192	0.7801	2.771492
v = 1.6 m/s	1.05823	0.41941	0.463068	0.825265	2.765973

Table 9 Conveying capacity statistics for the SGB800 middle trough

Velocity	Indirect transport volume (m^3/s)	Direct transport volume (m^3/s)	Total coal flow (t/h)
v = 0.8 m/s	0.87671	0.03974	2804.3627
v = 1.0 m/s	1.11867	0.04968	3575.1375
v = 1.2 m/s	1.30637	0.05962	4179.9074
v = 1.4 m/s	1.46284	0.06955	4689.1263
v = 1.6 m/s	1.61342	0.07949	5180.3102

Table 10 Conveying capacity statistics for the SGB1000 middle trough

Velocity	Indirect transport volume (m^3/s)	Direct transport volume (m^3/s)	Total coal flow (t/h)
v = 0.8 m/s	1.10753	0.05432	3555.2539
v = 1.0 m/s	1.38105	0.06790	4433.7723
v = 1.2 m/s	1.60679	0.08148	5166.1000
v = 1.4 m/s	1.82765	0.09505	5883.4708
v = 1.6 m/s	1.99896	0.10863	6449.2227

Table 11 Conveying capacity statistics for the SGB1250 middle trough

Velocity	Indirect transport volume (m^3/s)	Direct transport volume (m^3/s)	Total coal flow (t/h)
v = 0.8 m/s	1.49000	0.06624	4762.0934
v = 1.0 m/s	1.85979	0.08280	5944.3211
v = 1.2 m/s	2.16405	0.09936	6926.0280
v = 1.4 m/s	2.46013	0.11592	7882.6988
v = 1.6 m/s	2.76017	0.13248	8851.5150

Tables 7–9 were used as fitting samples. For each middle trough width, the scraper chain speed v was taken as the independent variable, and the total coal flow Q_{tot} was taken as the dependent variable. Since the velocity-domain areas S1–S4 vary with chain speed and the total coal flow consists of both the indirect conveying component and the direct scraper-pushing component, the relationship between Q_{tot} and v is not strictly linear. Therefore, a polynomial regression model was adopted to describe the nonlinear variation of coal flow with chain speed.

The coefficients of the fitting equations were obtained using the least-squares regression method, in which the sum of squared residuals between the fitted values and the calculated values was minimized. Based on this procedure, the coal flow calculation equations for the SGB800, SGB1000, and SGB1250 middle troughs were obtained as follows.

The total coal flow for the SGB800 middle trough, $Q_{tot\text{-}800}$, is given by the following equation:

$$Q_{tot800} = 565.463v^3 - 3241.034v^2 + 8179.152v - 1945.551 \quad (13)$$

The total coal flow for the SGB1000 middle trough, $Q_{tot\text{-}1000}$, is given by the following equation:

$$Q_{tot1000} = -454.538v^3 + 364.418v^2 + 4789.764v - 191.617 \quad (14)$$

The total coal flow for the SGB1250 middle trough, $Q_{tot\text{-}1250}$, is given by the following equation:

$$Q_{tot1250} = 2997.738v^3 - 11583.669v^2 + 19596.851v - 4896.750 \quad (15)$$

To further establish a unified calculation expression considering the influence of trough width, the middle trough width w and the scraper chain speed v were both introduced as independent variables. The data listed in Tables 7–9 were fitted using multivariable polynomial regression, and the unified fitting equation for the total coal flow Q_{tot} is expressed as

$$\begin{aligned} Q_{tot} = {} & 0.042w^2v^3 - 80.736wv^3 - 0.146w^2v^2 + \\ & 38261.640v^3 + 281.306wv^2 + 0.169w^2v - \\ & 134675.484v^2 - 321.648wv - 0.061w^2 + \\ & 157159.423v + 119.131w - 58010.522 \end{aligned} \quad (16)$$

where w is the middle trough width, (mm).

4.4 Coal flow calculation under different coal pile heights

To calculate the coal flow at different pile heights, the conveying cross-section was divided vertically, as shown in Figure 6. The same velocity-domain color definition as in Figure 3 was used in Figure 5; that is, the red, green, and yellow regions represent S_1, S_2, and S_3, respectively, while the uncolored region

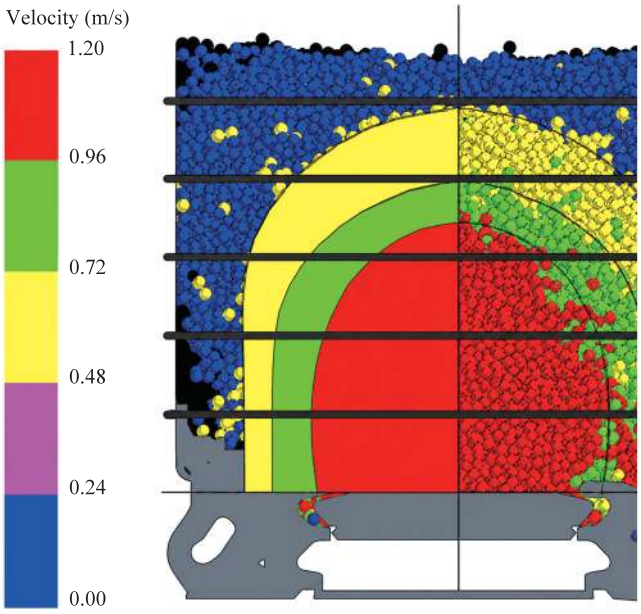

Figure 6 Vertical section division of the SGB1000 middle trough at a chain speed of 1.2 m/s

within the effective coal-flow cross-section represents S_4. Starting from the top surface of the scraper, the section was partitioned at 25 cm height intervals. The area of each sub-section was then measured, and the indirect transport volume for each layer was calculated using the formulas described above. Summing the contributions from all layers yields the total coal flow.

The calculation equation for the indirect transport volume at different coal pile heights is as follows:

$$V_{\text{mid-}h} = 0.9v \cdot S_{1h} + 0.7v \cdot S_{2h} + 0.5v \cdot S_{3h} + 0.3v \cdot S_{4h} \quad (17)$$

where S_{1h}–S_{4h} are the cross-sectional areas of the respective velocity domains at different coal pile heights.

The total coal flow can be calculated using the following equation:

$$Q_{\text{tot}} = \frac{\rho\left(V_{\text{mid-}h} + V_{\text{scr}}\right) \times 3600}{1000} \quad (18)$$

Tables 12–14 shows the coal flow rate (t/h) for different scraper speeds at various coal stacking heights in middle troughs of different widths.

The calculated coal flow values listed in Tables 10–12 were used as fitting samples for the cases with different coal pile heights. For each middle trough width, the scraper chain speed v and the coal pile height h were selected as independent variables, while the total coal flow $Q_{\text{tot-h}}$ was taken as the dependent variable. The calculated results show that coal flow increases with both chain speed and pile height, but the increase is nonlinear because the effective conveying area and the sectional velocity-domain distribution vary with the

Table 12 Coal flow (t/h) for different scraper speeds at various coal pile heights in the SGB800 middle trough

Height	Scraper speed v = 0.8 m/s	Scraper speed v = 1.0 m/s	Scraper speed v = 1.2 m/s	Scraper speed v = 1.4 m/s	Scraper speed v = 1.6 m/s
0.25 m	698.6102	912.7368	1116.5818	1309.9615	1480.4525
0.50 m	1313.0582	1688.1408	2068.7314	2408.8075	2688.7853
0.75 m	1871.4470	2419.4808	2902.2754	3339.7207	3686.5901
1.00 m	2312.3318	2983.7448	3537.5314	3989.6035	4430.7821
1.25 m	2667.0470	3409.6968	3981.4762	4481.8351	4983.0509
1.40m	2804.3627	3575.1375	4179.9074	4689.1263	5180.3102

Table 13 Coal flow (t/h) for different scraper speeds at various coal pile heights in the SGB1000 middle trough

Height	Scraper speed v = 0.8 m/s	Scraper speed v = 1.0 m/s	Scraper speed v = 1.2 m/s	Scraper speed v = 1.4 m/s	Scraper speed v = 1.6 m/s
0.25 m	834.2686	1110.1553	1316.7645	1568.7836	1694.9756
0.50 m	1569.4030	2045.9039	2422.0365	2858.2676	3117.2636
0.75 m	2282.0158	2928.7135	3477.7365	4043.2220	4435.2668
1.00 m	2895.7294	3650.5671	4311.6477	4939.4348	5416.9148
1.25 m	3341.9998	4200.7553	4887.0501	5594.4584	6136.1372
1.50 m	3555.2539	4433.7723	5166.1	5883.4708	6449.2227

Table 14 Statistics of coal flow rate (t/h) at different coal heap heights and scraper speeds for the SGB1250

Height	Scraper speed v = 0.8 m/s	Scraper speed v = 1.0 m/s	Scraper speed v = 1.2 m/s	Scraper speed v = 1.4 m/s	Scraper speed v = 1.6 m/s
0.25 m	1004.659	1348.5428	1591.4448	1771.4340	2148.3648
0.50 m	1935.878	2524.1948	2950.0848	3371.5080	3976.0416
0.75 m	2857.5504	3664.0440	4297.7088	4944.1644	5742.0288
1.00 m	3714.8400	4721.8865	5533.7040	6370.3080	7259.2992
1.25 m	4412.2752	5552.0642	6447.2976	7350.0588	8301.168
1.50 m	4762.0934	5944.3211	6926.028	7882.6988	8851.515

coal pile height. Therefore, a multivariable polynomial regression model was used to describe the combined influence of v and h on coal flow.

The fitting coefficients in Equations (18)–(20) were obtained by the least-squares method based on the calculated values in Tables 10–12. This method determines the coefficients by minimizing the difference between the fitted coal flow and the calculated coal flow under different combinations of chain speed and coal pile height.

The total coal flow for the SGB800 middle trough at varying coal pile heights, $Q_{\text{tot-}h\text{-}800}$, is given by the following equation:

$$\begin{aligned} Q_{\text{tot}-h-800} = {} & -139.003h^3 + 565.463v^3 - \\ & 1319.082h^2v - 831.518hv^2 + 580.709h^2 - \\ & 2076.910v^2 + 5845.070hv - 1174.026h + \\ & 2581.454v - 1058.679 \end{aligned} \tag{19}$$

where h is the coal pile height, (m).

The total coal flow for the SGB1000 middle trough at varying coal pile heights, $Q_{\text{tot-}h\text{-}1000}$, is given by the following equation:

$$\begin{aligned} Q_{\text{tot}-h-1000} = {} & -486.046h^3 - 454.538v^3 - \\ & 1507.626h^2v - 605.180hv^2 + 1534.398h^2 + \\ & 1272.188v^2 + 6132.272hv - 1536.542h - \\ & 1016.484v + 301.206 \end{aligned} \tag{20}$$

The total coal flow for the SGB1250 middle trough at varying coal pile heights, $Q_{\text{tot-}h\text{-}1250}$, is given by the following equation:

$$\begin{aligned} Q_{\text{tot}-h-1250} = {} & -1020.000h^3 + 2997.738v^3 - \\ & 1790.070h^2v - 773.776hv^2 + 3261.921h^2 - \\ & 10423.006v^2 + 8056.671hv - 3310.346h + \\ & 11539.502v - 3828.054 \end{aligned} \tag{21}$$

To obtain a generalized fitting formula applicable to different trough widths and coal pile heights, the middle trough width w, scraper chain speed v, and coal pile height h were introduced as independent variables. A multivariable polynomial regression was then performed using the calculated coal flow data of all three trough widths. The generalized fitting formula for $Q_{\text{tot-}h}$ is expressed as

$$\begin{aligned} Q_{\text{tot}-h-1250} = {} & -533.098h^2v^2 - 0.894wh^3 + \\ & 668.970v^3 + 113.765hv^2 + 3.335whv + \\ & 1.434wh^2 - 2700.287v^2 + 763.340hv + \\ & 3640.445v - 646.159h - 0.070w - \\ & 1375.578 \end{aligned} \tag{22}$$

To validate the effectiveness of the established coal flow fitting equations, the simulation results were compared with the predicted values from the formulas. The comparison shows that the fitted predictions agree well with the simulation results, with a maximum error percentage not exceeding 3%. This indicates that the fitted model has high computational accuracy and can reliably reflect the coal flow variations obtained from the discrete element simulations.

The discrete element simulations and fitted results in this study cover the commonly used middle trough widths in engineering (800–1250 mm) and typical chain speed ranges (0.8–1.6 m/s). Therefore, the established coal flow calculation models and fitting equations can satisfy the requirements for rapid estimation under mainstream specifications and operating conditions, providing a reliable basis for capacity boundary selection, operating condition constraints, and optimization of operational parameters.

4.5 Engineering significance and limitations of the proposed method

The proposed sectional velocity-domain method has practical engineering significance for scraper conveyor design and operation. First, it provides a rapid calculation approach for evaluating whether a given trough width, scraper chain speed, and coal pile height can satisfy the required conveying capacity. Compared with the traditional sectional average-velocity method, the proposed method considers the non-uniform contribution of different velocity regions to the total coal flow, thereby providing a more refined basis for capacity verification and operating parameter matching.

The method also provides indirect support for wear-risk analysis. The sectional velocity-domain results reflect the distribution of high-, medium-, and low-velocity coal flow regions in the middle trough. Low-velocity regions are usually associated with local accumulation and longer particle residence time, which may increase particle-structure contact and aggravate local wear. High-velocity regions may correspond to stronger particle impact and shear interaction. Therefore, the velocity-domain distribution can provide a reference for identifying regions where local accumulation, impact, or wear risks may be more likely to occur.

In practical operation, the calculated coal flow can support production and operation management. For a given scraper conveyor, the calculation model can be used to estimate the conveying capacity under different chain speeds and coal pile heights, providing a basis for selecting suitable operating parameters. Underestimation of coal flow may reduce production efficiency, whereas overestimation may lead to overload, abnormal accumulation, and increased energy consumption. Therefore, the proposed method can help balance conveying capacity, operating stability, and equipment safety.

From the perspective of economic performance, the method may help reduce unnecessary equipment oversizing, overload operation, and unplanned downtime by improving the accuracy of coal flow estimation and parameter matching. However, this study does not provide a quantitative cost-benefit estimation because detailed field data, such as maintenance cost, downtime loss, energy consumption records, and production value, were not available. Future work will combine the proposed coal flow calculation model with field operation data to further evaluate its quantitative economic benefits.

In addition, the proposed coal flow calculation model can provide a calculation basis for intelligent monitoring of scraper conveyors. In practical operation, online signals such as scraper chain speed, motor current, load state, and coal pile height can be used as monitoring inputs. By comparing the estimated coal flow state with the expected conveying capacity, abnormal conditions such as local accumulation, overload, or insufficient conveying capacity may be identified. Therefore, the present study does not directly develop an intelligent monitoring system, but provides a calculation basis for coal flow state estimation and subsequent monitoring applications.

5 Experimental validation

To verify the coal-flow calculation method proposed in this study, a scaled experiment was conducted using a 1:2 scaled SGB1000 scraper conveyor test rig. The geometric similarity ratio of the scaled platform was λ = 0.5. The experimental system consisted of the scaled middle trough, scraper chain, drive system, and coal-retaining baffles. The baffles were installed on both sides of the trough to maintain a stable coal accumulation state and to ensure consistency with the DEM boundary conditions. The physical setup of the experimental platform is shown in Figure 7.

During the experiment, the scraper chain was operated at the specified chain speed until the coal flow

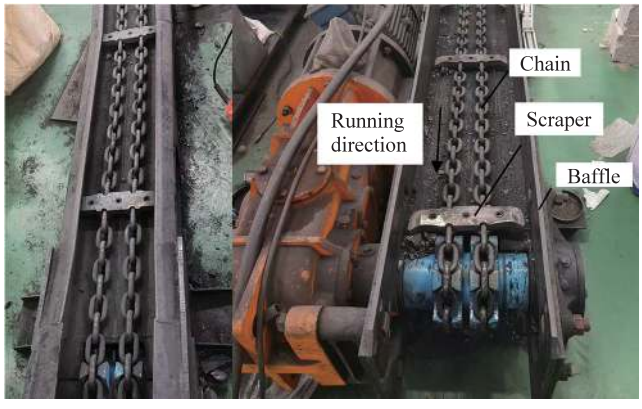

Figure 7 Physical setup of the experimental rig

reached a stable conveying state. The discharged coal mass within a fixed time interval was measured, and each working condition was repeated three times. The average value was used as the experimental coal flow rate.

To verify the output of the DEM-based coal-flow prediction functions established in Sections 4.2 and 4.3, four representative validation conditions were selected. The scaled coal pile heights were 0.150 and 0.250 m, corresponding to prototype coal pile heights of 0.300 and 0.500 m, respectively. For each height, two scraper chain speeds of 1.0 and 1.4 m/s were adopted. The comparison results are shown in Table 15.

As shown in Table 15, the predicted coal flow rates agree well with the prototype-equivalent experimental results. The coal flow rate increases with increasing coal pile height and scraper chain speed in both the predicted and experimental results. The relative errors of the four validation conditions are within 10%, with a maximum error of 8.96%. This indicates that the DEM-based coal-flow prediction functions established in Sections 4.2 and 4.3 can reasonably predict the coal flow under different working conditions.

6 Conclusions

(1) A coal flow calculation method based on sectional velocity domain statistics was proposed. By transforming the complex non-uniform velocity field into quantifiable domain areas and representative velocities, the method achieves a refined calculation of coal flow.

(2) The influence of middle trough width, scraper chain speed, and coal pile height on coal flow was systematically analyzed. A fitting equation for coal flow suitable for mainstream scraper conveyor models was established, offering high calculation accuracy and covering the main specifications and common operating conditions.

(3) The proposed calculation method for coal flow was validated through scaled experiments. The experimental results were generally consistent with the calculated results, confirming the effectiveness and engineering applicability of the method.

(4) The proposed method provides an equivalent coal flow estimation model for scraper conveyor capacity verification, operating parameter matching, and overload risk assessment. When combined with online measurements such as scraper chain speed, motor current, load state, and coal pile height, the model may further provide a calculation basis for coal flow state estimation and intelligent monitoring of scraper conveyors.

Acknowledgements

This research was financially supported by the Key Program of the National Natural Science Foundation of China (No. 52234005) and the Taishan Scholars Program of Shandong Province (No. tstp20250532).

Author contributions

xxxx.

Data availability

xxxx.

Declaration of competing interest

The authors declare that they have no known competing financial interests or personal relationships that could have appeared to influence the work reported in this paper.

Table 15 Comparison between predicted coal flow and scaled experimental results

Case No.	Scaled coal pile height, h_s (m)	Prototype coal pile height, h (m)	Chain speed, v (m/s)	Formula-predicted coal flow, Q_{cal} (t/h)	Scaled formula-predicted flow, $Q_{cal,s}$ (t/h)	Scaled experimental flow, Q_{exp} (t/h)	Error (%)
1	0.25	0.5	1	2512.92	628.23	596.7	5.02
2	0.25	0.5	1.4	3411.6	852.9	815.38	4.4
3	0.30	0.6	1	2979.26	744.82	686.04	7.89
4	0.30	0.6	1.4	4047.16	1011.79	1102.46	8.96

References

[1] Lubenets, T. M., Koroviaka, Y. A., Snigur, V. H., Tkachuk, A. V., and Rastsvietaiev, V. O. "Theoretical model of random freight flow distribution in the conveyor transport line of the coal mine," *Scientific Bulletin of National Mining University*, no. 6, 2023.

[2] Nikitenko, S. M., Khudyntsev, E. A., Kizilov, S. A., and Korolev, M. K. "Outlet facility to pass coal flow to armored face conveyor," *IOP Conference Series: Earth and Environmental Science*, vol. 823, no. 1, 2021.

[3] Bahrun, S., Yusoff, M. S., Said, M. S., and Hassan, A. "Coal flowability control on preventing spillage on conveyor belt through modeling and simulation for improving its performance," *Journal of Advanced Research in Fluid Mechanics and Thermal Sciences*, vol. 90, pp. 130, 2022.

[4] Li, S., Zhu, Z., Lu, H., and Xue, Y. "Tension characteristics analysis of scraper chain of heavy-duty scraper conveyor with time-varying loads," *Shock and Vibration*, vol. 2024, no. 1, 2024.

[5] Zhang, X., Ren, M., Wang, H., and Jin, L. "Simulation study on dynamic characteristics of the chain drive system for mining scraper conveyor driven by the permanent magnet synchronous motor," *Processes*, vol. 12, no. 1, 2024.

[6] Jiang, S., Ren, W., Mao, Q., Zeng, Q., Yu, P., Gao, K., and Wang, L. "Dynamic analysis of the scraper conveyor under abnormal operating conditions based on the vibration and speed characteristics," Shock and Vibration, vol. 2021, no. 1, Art. no. 8887744, 2021.

[7] Xie, C., Liu, Z., and Xie, M. "Dynamic response analysis of scraper conveyor under the condition of chain broken," *Journal of Vibroengineering*, vol. 25, no. 6, pp. 1053, 2023.

[8] Shprekher, D. M., Ovsyannikov, D. S., and Zelenkov, A. V. "Dynamic analysis of the reaction of a scraper conveyor when a chain is jammed," in *2024 International Conference on Industrial Engineering, Applications and Manufacturing (ICIEAM)*, pp. 983–989, 2024.

[9] Wang, Z., Li, B., Liang, C., Wang, X., and Li, J. "Response analysis of a scraper conveyor under chain faults based on MBD-DEM-FEM," *Strojniški Vestnik—Journal of Mechanical Engineering*, vol. 67, no. 10, pp. 501–515, 2021.

[10] Xia, R., Wang, X., Li, B., Wei, X., and Yang, Z. "The prediction of wear on a scraper conveyor chute affected by different factors based on the discrete element method," *Proceedings of the Institution of Mechanical Engineers, Part C: Journal of Mechanical Engineering Science*, vol. 233, no. 17, pp. 6229–6239, 2019.

[11] Ilic D ,Lavrinec A ,Orozovic O . "Simulation and analysis of blending in a conveyor transfer system," *Minerals Engineering*, vol. 157, 2020.

[12] Ilic, D., Roberts, A., Wheeler, C., and Katterfeld, A. "Modelling bulk solid flow interactions in transfer chutes: Shearing flow," *Powder Technology*, vol. 354, pp. 30, 2019.

[13] Ilic, D., Lavrinec, A., and Orozovic, O. "Simulation and analysis of blending in a conveyor transfer system," *Minerals Engineering*, vol. 157, Art. no. 106529, 2020.

[14] Zhu, H. P., Zhou, Z. Y., Yang, R. Y., and Yu, A. B. "Discrete particle simulation of particulate systems: Theoretical developments," *Chemical Engineering Science*, vol. 62, no. 13, pp. 3378–3396, 2007.

[15] Wang X, Li B, Yang Z. "Analysis of the bulk coal transport state of a scraper conveyor using the discrete element method," *Strojniški Vestnik—Journal of Mechanical Engineering*, vol. 64, no. 1, 2018.

[16] Wang, Z., Li, B., Liang, C., Wang, X., and Li, J. "Response analysis of a scraper conveyor under chain faults based on MBD-DEM-FEM," *Strojniski Vestnik—Journal of Mechanical Engineering*, vol. 67, no. 10, pp. 501, 2021.

[17] Xia, R., Wang, X., Li, B., Wei, X., and Yang, Z. "The prediction of wear on a scraper conveyor chute affected by different factors based on the discrete element method," *Proceedings of the Institution of Mechanical Engineers, Part C: Journal of Mechanical Engineering Science*, vol. 233, no. 17, pp. 6229, 2019.

[18] Liu, H., Liu, Z., Wang, X., and Wang, M. "Analysis of wear characteristics of coal particles with different particle sizes in the middle trough of a scraper conveyor," in *Fourth International Conference on Advanced Manufacturing Technology and Electronic Information (AMTEI 2024)*, SPIE, 2025, vol. 13515, pp. 238.

[19] Xia, R., Wang, X., Li, B., Wei, X., and Yang, Z. "Discrete element method- (DEM-) based study on the wear mechanism and wear regularity in scraper conveyor chutes," *Mathematical Problems in Engineering*, vol. 2019, 2019.

[20] Ma, H., Wang, X., Li, B., Liu, Z., Bi, W., and Wei, X. "Study on the mechanical effect and wear behaviour of middle trough of a scraper conveyor based on DEM–MBD," *Proceedings of the Institution of Mechanical Engineers, Part J: Journal of Engineering Tribology*, vol. 236, no. 7, pp. 1363, 2022.

[21] Yanping Y ,Weili L ,Zhipeng G . "Impact damage to the middle trough of a scraper conveyor based on the engineering discrete element method and orthogonal matrix analysis," *PLOS ONE*, vol. 17, no. 4, Art. no. e0266831, 2022.

[22] Wang, X., Li, B., Wang, S., Yang, Z., and Cai, L. "The transporting efficiency and mechanical behavior analysis of scraper conveyor," *Proceedings of the Institution of Mechanical Engineers, Part C: Journal of Mechanical Engineering Science*, vol. 232, no. 18, pp. 3315, 2018.

[23] Zhang, P., Li, B., Wang, X., Liu, C., Bi, W., and Ma, H. "The loading characteristics of bulk coal in the middle trough and its influence on rigid body parts," *Strojniški Vestnik—Journal of Mechanical Engineering*, vol. 66, no. 2, pp. 114, 2020.

[24] CUNDALL P A, STRACK O D L. A discrete numerical model for granular assemblies[J]. *Géotechnique*, 1979, 29(1): 47–65.

[25] Cundall, P. A., and Strack, O. D. L. "A discrete numerical model for granular assemblies," *Géotechnique*, vol. 29, no. 1, pp. 47–65, 1979.

[26] Kwok C Y, Bolton M D. "DEM simulations of thermally activated creep in soils," *Géotechnique*, vol. 60, no. 6, pp. 425, 2010.

[27] Jelinek B, Card A, GL. Mason, K Grebner, A Dickerson, T Skorupa, M Cole, JD. Priddy, "Tractive performance of rigid wheel in granular media using coarse-scale DEM models," *Journal of Terramechanics*, vol. 117, Art. no. 101016, 2025.

[28] L. Zhang, "Analysis of Scraper Conveyor Transporting Coal Powder Based on Discrete Element Method," M.S. Dissertation, Taiyuan University of Technology, Taiyuan, China, 2015.

[29] Ren, J., Wang, Q., and Liu, Z. "Analysis calculation of scraper conveyor transport capacity," *Coal Mine Machinery*, vol. 34, no. 3, pp. 30–31, 2013.